Flow and jamming of a two-dimensional granular bed: Toward a nonlocal rheology?

Lydie Staron,[a] Pierre-Yves Lagrée, Christophe Josserand, and Daniel Lhuillier
CNRS UMR7190-Université Pierre et Marie Curie, IJLRDA, 4 place Jussieu, 75252 Paris, France

(Received 4 February 2010; accepted 20 September 2010; published online 11 November 2010)

In order to test the rheology of granular flows, we performed series of numerical simulations of nearly monodisperse stationary chute flows from rapid to slow and very slow flow regime, namely, close to the jamming transition. We check how existing rheological models (i.e., Bagnold's model and the *I*-model) capture the behavior of the numerical flows, and perform an acute characterization of the structure of the flow in terms of grains velocity fluctuations close to the jamming transition. The simulations show that both Bagnold's and the *I*-model fail to describe the data points in the slow regime, namely, when $I \leq 2 \times 10^{-2}$. Turning to the analysis of grains velocity fluctuations, we compute the associated correlation length λ and show its dependence on the inertial number: $\lambda/d \propto I^{-0.32}$. The amplitude of the grains velocity fluctuations, namely, the granular temperature, exhibits a power-law dependence on the shear rate and allows for an efficient prediction of the shape of the velocity profiles. The main result consists of a scaling merging all data points for all flow regimes onto the same master curve, and relating granular temperature, shear rate, and the variation of stress between the considered depth and the bottom wall. This scaling can be written as a relation between local stress, local shear rate, and local temperature, provided the introduction of a characteristic length scale $\xi = d\sqrt{(H-z)/z}$ where both the distance to the surface and the distance to the bottom wall are involved. This scaling strongly suggests a nonlocal behavior, valid in the flow regime and extending close to the jamming transition, and hints at granular temperature as the variable at the origin of the nonlocality. © *2010 American Institute of Physics*.
[doi:10.1063/1.3499353]

I. INTRODUCTION

In spite of their huge importance in natural processes (catastrophic flows, erosion, and transport) and in human activity (industrial handling and geotechnics), granular flows escape in a large extent understanding and thus theoretical modeling. Oddly enough, systems as simple as stationary monodisperse flows on rough inclines still present many unexplained features: the relation between flow depth and angle of avalanche, the nature of the relation between the correlated motion of grains and the macroscopic properties, the hysteretic behavior around the flow and arrest transition, the influence of the nature of the substrate, etc.[1–6] The underlying question, indeed, is the actual rheology of the flow and its robustness regarding boundary conditions.

Among the various models proposed for modeling granular flows, a recurrent issue is the definition of a variable, or of an order parameter, that would allow for the discrimination between the static ("solidlike") and flowing ("fluidlike") species of grains, and their respective contribution to the total stress state.[7–10] While volume fraction stands as the most relevant variable for the description of dense flow regimes, for which kinetic theory is no longer applicable, the definition of a univocal relation between rheological properties such as friction or viscosity and volume fraction remains a challenge.

The Bagnold rheology, beyond Bagnold's analysis of collisional flows phenomenology, emerges from dimensional analysis considering that there are no characteristic length and time scales in a granular flow other than the grain diameter and the inverse of the shear rate. In this framework, the effective viscosity of the flow is proportional to the shear rate, and diverges when the volume fraction reaches close to the critical value for which jamming occurs. Drawing an analogy with the Prandtl mixing length in turbulent flow, the divergence of the viscosity can be interpreted as the emergence of a coherence length in the system related to the existence of clusters (or "eddies") of correlated grains.[11] This was supported by experimental and numerical observation of correlated motion of grains in granular chute flows.[6,12–14] However, the divergence of the viscosity and the evolution of the correlation length are poorly characterized.

Lately, the inertial number *I* has opened a new path by merging along a single phenomenological law many experimental data as well as numerical works, even in highly transient and inhomogeneous situations.[15–17] Defined as the ratio of the typical time of macroscopic deformation to the typical time of local rearrangements,[15,16,18,19] *I* can be seen as the long-sought order parameter allowing for the unambiguous characterization of the state of the packing. Eventually, the *I* rheology has emerged as the only framework so far reconciling flow data and experimental settings which before seemed manyfold and quite disparate.[20]

However, in spite of this progress, the transition toward slow flow regime and ultimately jamming remains problem-

[a]Electronic mail: staron@lmm.jussieu.fr.

atic. For instance, the origin of the relation between flow depth and the angle of avalanche is a well-known difficulty left unsolved by the various propositions for a rheology.[1] Sharp localization, or on the contrary creep motion under avalanches at the surface of a heap, cannot be captured in the framework of the I rheology.

Behind these unexplained features, a more fundamental issue is raised: does the assumption of a local rheology allow for a comprehensive description of granular media?[21–23] The existence of an intermediate "mesoscopic" scale related to force transmission led to the suggestion that force chains might be at the origin of nonlocal behavior.[22] In the same way, the existence of correlated motion of grains and the role of these "granular eddies" in the macroscopic behavior could be reconsidered from this point of view.[6,11–13] Recently, a proposition of nonlocal rheology has been proven successful in giving account of experimental features so far escaping modeling,[23] and strongly suggests that the assumption of a local rheology is too simplistic. The question is now, which mechanisms, linked to which variables, are likely to result in nonlocality?

In this contribution, we try to bring new insights in these issues by carefully analyzing two-dimensional (2D) simulations of chute flows, from relatively rapid to slow and very slow flow regimes. Computing velocity field and stress state locally, we try out Bagnold model and the I-model, and find that the frameworks they provide fail to capture the behavior of the simulations in the limit of slow flow regimes. Turning to a Prandtl-like approach, we study grains velocity fluctuations, and characterize the emergence of a correlation length and its divergence as a function of the inertial number I. We then focus on granular temperature and its profiles; we show its relation to velocity gradients and derive an expression for velocity profiles matching the data. Looking for a relation between effective viscosity and temperature, we find that the only scaling merging all simulation points on a single curve relates the stress, the shear rate, and the granular temperature while implying the existence of a length scale involving the flow depth and the distance to the bottom. This observation strongly suggests a nonlocal behavior and hints at granular temperature as the variable at the origin of the nonlocality.

II. NUMERICAL GRANULAR STATIONARY FLOWS

A. Algorithm and setup

The numerical method applied is the nonsmooth contact dynamics.[24,25] Each grain obeys the equations of dynamics for translational and rotational velocities, taking into account external forces (in our case gravity) and the forces applied by neighboring grains through contacts. Contact forces are solved implicitly on the basis of two nonsmooth contacts laws, namely, Coulombic friction and a strict condition of nonoverlap. The friction law prescribes the maximum value of the tangential force T, given by the Coulomb threshold $\mu_c N$, where N is the normal force at contact, and μ_c is the microscopic coefficient of friction at contact. Once this threshold is attained, slip motion can occur and energy thus be dissipated. The microscopic coefficient of friction μ_c sets the value of the Coulomb threshold and the efficiency of dissipation due to slip motion.

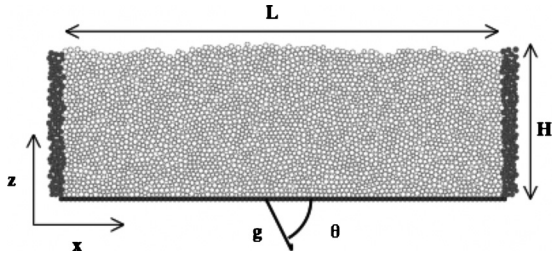

FIG. 1. Example of a 2D granular bed simulated by contact dynamics. The direction of the flow is denoted x, the direction normal to the flow is denoted z and is counted positively in the upward direction, H is its thickness, L its lateral extension, and θ the slope.

An additional source of energy dissipation is the inelastic restitution of energy during collisions; the coefficient of restitution e sets the efficiency of the dissipation. This algorithm has proven reliable in both quasistatic and dynamical situations, for which experimental findings are recovered with good agreements.[6,26]

The setup simply consists of 2D granular beds made of circular beads with slightly different diameters (i.e., such that $d_{\max}/d_{\min}=1.5$), the mean diameter being denoted d. The beds are created by random deposition of grains in the gravity field. The bottom is made of glued grains of diameter d, showing the same properties μ_c and e as the free grains. The simulation cell is periodic in the x direction, allowing for stationary flow regimes; their lateral extension is $L=100d$. The direction normal to the flow is z and the height of the beds is denoted H (see Fig. 1). The beds are tilted of an angle θ for which stationary flow develops after a transient regime. To reach very small values of inertial number I (where $I=d(\partial v_x/\partial z)/\sqrt{P/\rho}$, see Sec. III), the slope θ was decreased gradually until no stationary flow was any longer possible.

Three sets of simulations were carried out. The first set, referred to as set A in the following, consists of beds counting 4000 grains ($H\simeq 38d$, $L=100d$) with a microscopic coefficient of friction $\mu_c=0.1$ and a coefficient of restitution $e=0.9$. These values coincide with low dissipation and favor flowing even for small θ, thus permitting to explore small values of I for which the flow reaches regimes very close to arrest. Close to flow arrest, the reproducibility is expected to be low, so that four independent simulations were performed for each value of θ. The latter was varied in the interval $[14°,16°]$.

The second set of simulations, referred to as set B, consists of beds counting 3200 grains ($H\simeq 31d$, $L=100d$) with a coefficient of restitution $e=0.5$ and a microscopic coefficient of friction $\mu_c=0.3$. These values coincide with highly dissipative properties, thus preventing the bed to reach low value of I. The slope interval covered is $[16°,26°]$. The third set of simulation, referred to as set C, shows the same geometry as set B. The coefficient of restitution is $e=0.5$ and the microscopic coefficient of friction is chosen very low $\mu_c=0.01$, which allows for low values of the inertial number I. The slope interval covered is $[10.5°,19°]$.

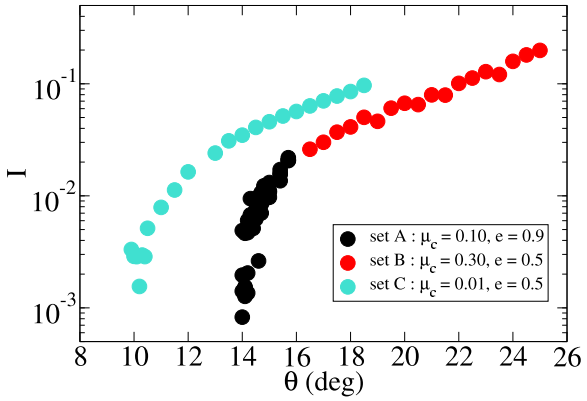

FIG. 2. (Color online) Mean inertial number I as a function of the slope θ for all simulations from sets A, B, and C. Each point coincides with one simulation.

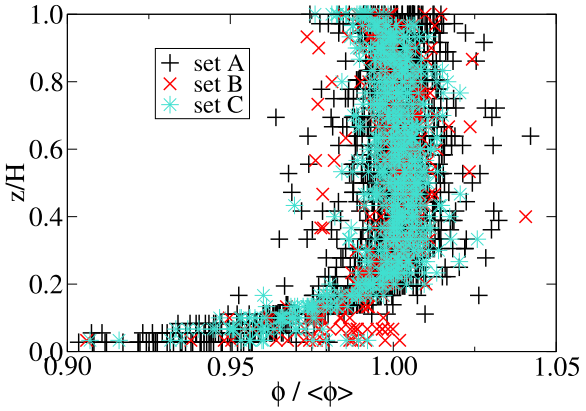

FIG. 3. (Color online) Normalized profiles of the volume fraction $\phi(z)/\langle\phi\rangle$ for all simulations from sets A, B, and C, where $\langle\phi\rangle$ is the mean volume fraction over the flow volume.

A total of 90 runs were carried out, of a duration $T \simeq 70\sqrt{d/g}$, with $d=0.05$ m, namely, 5000 time steps of 10^{-3} s. In the following, all quantities computed are averaged over the simulations duration.

For the three sets of simulations, the global value of the inertia number I is plotted as a function of the slope θ in Fig. 2: the simulations cover two orders of magnitude for I and reach close to jamming. The aim in testing different grains properties is not to carry a parametric study, but rather to assess the robustness of the results discussed hereafter regarding "microscopic" details. In the following, all graphs show the simulation points from sets A, B, and C; although visually differentiated, they will not be systematically discussed separately. A summary of the simulations performed and the corresponding parameters is given in Table I.

B. Analysis of the simulations

1. Volume fraction

The volume fraction ϕ is defined as the ratio of the volume of the grains to the volume of the packing

$$\phi = \frac{V_{\text{grains}}}{V_{\text{packing}}}.$$

When computing the mean volume fraction over the whole flow, the free surface is an obvious source of uncertainty: its uneven shape results in error in the evaluation of the volume of the packing. For this reason, the mean volume fraction was always computed in the bulk excluding the three first layers of grains under the free surface. For our simulations, the mean volume fraction varies between 0.715 and 0.795.

For all simulations of sets A, B, and C, we compute the volume fraction profiles $\phi(z)$ by dividing the beds in layers of thickness d. These profiles are reported in Fig. 3 normalized by the mean value of the volume fraction $\langle\phi\rangle$. The case $z=1d$ corresponds to the first layer immediately after the bottom. We observe that the volume fraction shows only slight variations throughout the bulk, but that a systematic dip occurs close to the bottom: the rigid bottom locally induces agitation and thereby a decompaction of the packing. Although this effect is enhanced by high values of the coefficient of restitution (set A of simulations), it is as well visible for lower values (sets B and C). Similar behavior is observed for vertically shaken granular layers, and was identified as an analogous of the Leidenfrost effect.[27] It is interesting that this effect endures in the case of slow to very slow chute flows.

2. Stress tensor

The stress tensor $\boldsymbol{\sigma}$ is defined as the sum of two contributions: the static stress tensor $\boldsymbol{\sigma}^c$ related to the contact forces, and the Reynolds tensor $\boldsymbol{\sigma}^r$ related to the grains velocity fluctuations.

These contributions are defined as follows:

$$\boldsymbol{\sigma}^c = \frac{1}{V}\sum_{\alpha} \vec{f}^{\alpha} \otimes \vec{r}^{\alpha},$$

where $\vec{f}$ and $\vec{r}$ are, respectively, the force transmitted at contact α and the vector joining the two centers of mass of the grains involved in the contact, and where V is the volume over which the summation is made;

TABLE I. Table of simulations performed.

Simulations	N grains	L	H	e	μ_c	Range of θ	Range of I	N runs
Set A	4000	100 d	38 d	0.9	0.1	[14°, 16°]	$[8\times10^{-4}, 1.5\times10^{-1}]$	52
Set B	3200	100 d	31 d	0.5	0.3	[16°, 26°]	$[2.5\times10^{-2}, 2.8\times10^{-1}]$	20
Set C	3200	100 d	31 d	0.5	0.01	[10°, 19°]	$[4.6\times10^{-3}, 10^{-1}]$	18

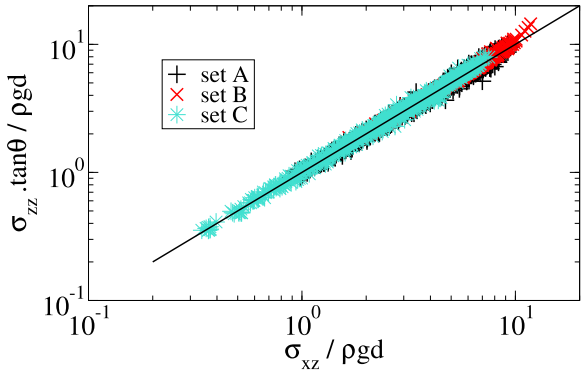

FIG. 4. (Color online) Normalized stress component $\sigma_{zz}\tan\theta/\rho gd$ as a function of the normalized stress component $\sigma_{xz}/\rho gd$ computed at each depth z for all simulations from sets A, B, and C. The solid line has slope 1.

$$\boldsymbol{\sigma}^r = \frac{1}{V}\sum_i m_i \delta\vec{v}_i \otimes \delta\vec{v}_i,$$

where $\delta\vec{v}_i$ is the velocity fluctuation of the grain i. In the simulations discussed in the paper, the contribution of the static stress tensor is dominating.

Computing the stress profile for all simulations $\sigma_{xz}(z)$ and $\sigma_{zz}(z)$, we check that everywhere in the flow, we recover the relation $\sigma_{xz}/\sigma_{zz}=\tan(\theta)$ expected from the force balance (Fig. 4); therefore in the following, we will mainly consider the σ_{zz} component, even for the computation of the effective viscosity. Moreover, we also check that $\sigma_{zz}=P\simeq\rho g(H-z)\cos\theta$. In this flow configuration, the stress tensor is found parallel to the flow, namely, to the strain tensor.

III. THE BAGNOLD RHEOLOGY

The Bagnold scaling is the rheology most widely accepted for granular flows on inclines, and the only one emerging from dimensional analysis considering that there are no other intrinsic length and time scale beside those prescribed by the grains diameter and the shear rate. In this framework, the divergence of the effective viscosity is related to the divergence of a "viscosity function" K through the relation

$$\boldsymbol{\sigma} = \rho d^2 K(\phi)\|\dot{\gamma}\|\dot{\gamma}, \tag{1}$$

where $\dot{\gamma}$ is the strain rate and where K diverges when ϕ tends toward the critical value ϕ_M. In this section, we investigate how the simulations fit in the Bagnold rheology.

A. Divergence of the viscosity

Transposed to our flow configuration, the Bagnold scaling reads

$$\sigma_{zz} = \rho d^2 \kappa(\phi)\left(\frac{\partial v_x}{\partial z}\right)^2 \tag{2}$$

and $\eta=\rho d^2\kappa(\phi)\,\partial v_x/\partial z$ is the viscosity. Close to flow arrest, the volume fraction ϕ increases toward a maximum, or critical value ϕ_M for which the system jams, and relative motion of grains is no longer possible. This coincides with an infinite value of the effective viscosity, that is, with the divergence of the viscosity function κ when $\phi\to\phi_M$. In the following, we try to specify the shape of $\kappa(\phi)$.

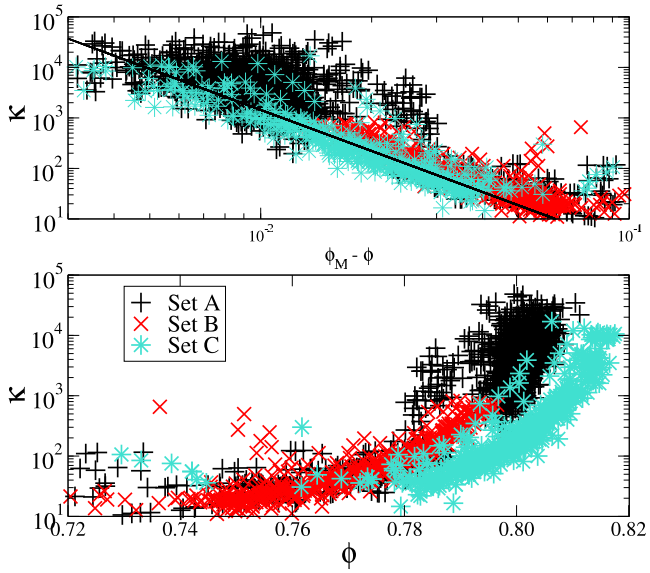

FIG. 5. (Color online) Viscosity function κ, defined as $\kappa=\sigma_{zz}/\rho d^2(\partial v_x/\partial z)^2$, computed at each depth z and plotted as a function of the volume fraction $\phi(z)$ for all simulations from sets A, B, and C. Top graph: viscosity function κ as a function of $\phi_M-\phi(z)$; the full line shows $\kappa=0.056(\phi_M-\phi)^{-2.7}$.

Computing σ_{zz} and the shear rate $\partial v_x/\partial z$ locally at all depths z for all simulations, we evaluate $\kappa=\sigma_{zz}/\rho d^2(\partial v_x/\partial z)^2$. We plot κ as a function of the local volume fraction $\phi(z)$ in Fig. 5. As expected we observe a function rapidly diverging when ϕ tends toward its maximum value ϕ_M. The value of ϕ_M appears to be dependent on the contact friction μ_c. We search for a fit of the form $\kappa=(\phi_M-\phi)^\beta$. For sets B and C, we are able to determine the value of ϕ_M which allows for the better data collapse (namely, respectively, $\phi_M=0.815$ and $\phi_M=0.825$). Fitting all simulation points together, the best fit approximation gives $\beta=2.73\pm0.07$ (with a correlation coefficient of 0.88). However, the value of β is very sensitive to the choice of ϕ_M, and varies between 2.6 and 3 for ϕ_M varied of ±0.003, with the correlation coefficient not degrading under 0.85. Thus, $\beta\simeq2.73$ remains a rough estimate. This value is compatible with what was observed numerically by Ref. 15. While important scattering occurs for $\phi\to\phi_M$, the points from simulation set A can hardly be fitted at all by a power-law.

Eventually, we find it impossible to characterize the shape of viscosity function close to the jamming transition. In this range, the volume fraction ϕ does not seem a sufficient variable to describe the divergence of the viscosity.

B. Volume fraction and inertial number

Alternatively to the volume fraction ϕ, the inertial number I has emerged as a powerful description of the state of granular flows, capturing the behavior of frictional properties as well as the evolution of the packing compaction.[15,16,20] In our flow configuration, the inertial number I is defined as

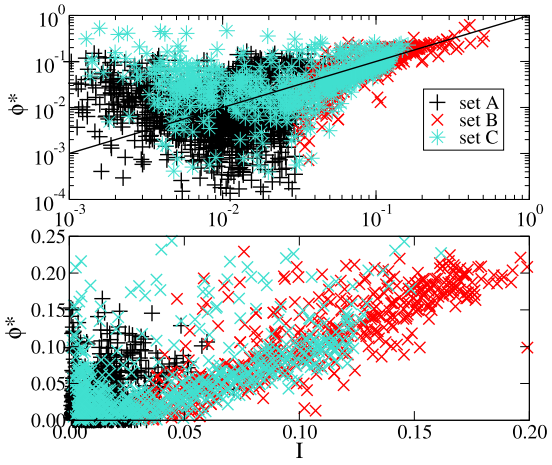

FIG. 6. (Color online) Reduced volume fraction $\phi^\star(z)$ (see text) as a function of the inertial number $I(z)$ computed locally at different depth z for all simulations from sets A, B, and C, in linear and log-log scales; the full line shows $\phi^\star = I$.

$$I = \frac{d(\partial v_x/\partial z)}{\sqrt{P/\rho}},$$

where ρ is the mass density of the grains, d their mean diameter, and P the pressure.[16] In relation to the volume fraction, it was suggested that[15]

$$\phi = \phi_M + (\phi_m - \phi_M)I,$$

where ϕ_m and ϕ_M are material dependent parameters: ϕ_M is the value of the volume fraction at rest, while ϕ_m represents the limit value of the volume fraction for a highly dynamic situation. On the basis of these findings, we search for a linear dependence between the local volume fraction $\phi(z)$ and the inertial number $I(z)$

$$\phi(z) = \phi_M + (\phi_m - \phi_M)I(z), \tag{3}$$

where

$$I(z) = \frac{d(\partial v_x/\partial z)(z)}{\sqrt{P(z)/\rho}}. \tag{4}$$

The best fit approximation gives $\phi_m = 0.494$ and $\phi_M = 0.661$ for set B (with a correlation coefficient of 0.88) and $\phi_m = 0.582$ and $\phi_M = 0.810$ for set C (with a correlation coefficient of 0.84). For simulation set A, a linear fit is hardly possible at all, but would give $\phi_m = 0.292$ and $\phi_M = 0.802$ (with a correlation coefficient of 0.3). Using these values, we plot the reduced volume fraction $\phi^\star(z) = [\phi_M - \phi(z)]/(\phi_M - \phi_m)$ as a function of $I(z)$ in a log-log scale (Fig. 6). The expected linear trend might be acceptable for the largest values of I, but the large scattering for smaller I makes it impossible to derive any clear relation between ϕ and I.

(Note that this is consistent with the behavior of $\kappa(\phi)$. Indeed, by definition [Eq. (2)], and considering that $P = \sigma_{zz}$ for the simulated flows (see Sec. II), $\kappa = I^{-2}$. Hence, a linear relation between $(\phi_M - \phi)$ and I would lead to $\kappa(\phi) \propto (\phi_M - \phi)^{-2}$, and contradict the observed scaling $\kappa(\phi) \propto (\phi_M - \phi)^{-2.7}$).

IV. THE *I* RHEOLOGY

Rather than focusing on the viscosity, whose divergence makes the characterization of incipient jamming difficult, we now consider the evolution of frictional properties. In this section, we study the effective coefficient of friction of the flows, and investigate its relation to the inertial number I, following earlier works and the proposition of the "I rheology."[16,20,28] More specifically, we explore the limit $I \to 0$.

A. The frictional properties

At all depths in the flow, we compute the local value of the coefficient of friction $\mu(z)$ as the ratio of the tangential component to the normal component of the stress tensor:

$$\mu(z) = \sigma_{xz}(z)/\sigma_{zz}(z). \tag{5}$$

As expected we observe $\mu(z) \simeq \tan(\theta)$ (see Fig. 4), where θ is the slope of the flow, and $\mu(z)$ is constant all through the bulk.

We search for a relation between friction and inertial number of the form:[28]

$$\mu(z) = \mu_m + \frac{\mu_M - \mu_m}{I_0/I(z) + 1}, \tag{6}$$

where μ_m, μ_M, and I_0 are material-dependent parameters to be determined; μ_m gives the value of the friction for a bed at rest, while μ_M set the value of the friction for larger I, together with I_0 and μ_m. The best fit approximation gives $\mu_m \simeq 0.256$, $\mu_M \simeq 0.496$, and $I_0 = 0.134$ for set A (again with a very poor correlation coefficient), $\mu_m \simeq 0.256$, $\mu_M \simeq 0.680$, and $I_0 = 0.24$ for set B (with a correlation coefficient of 0.88), and $\mu_m \simeq 0.171$, $\mu_M \simeq 0.615$, and $I_0 = 0.237$ for set C (with a correlation coefficient of 0.87).

In the following, rather then considering μ, we form the *reduced coefficient of friction* $\mu^\star$

$$\mu^\star = \frac{\mu(z) - \mu_m}{\mu_M - \mu(z)}. \tag{7}$$

Satisfying relation (6) implies $\mu^\star = I/I_0$. As can be seen in Fig. 7 where $\mu^\star$ is plotted as a function of I/I_0, this is mostly the case. However, if the linear dependence holds for the larger values of the inertial number, the large scattering observed for the smaller values ($I < 2 \times 10^{-2}$) makes any relation between effective friction and inertial number very uncertain in this range.

Note that similar conclusions were drawn in Ref. 21; however this was the result of the finite value of the stiffness of the grains; in the present case, grains are infinitely rigid (which is an intrinsic feature of the nonsmooth contact dynamic method).

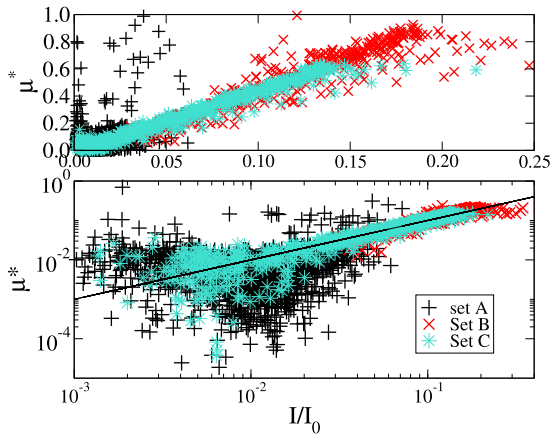

FIG. 7. (Color online) Reduced coefficient of friction $\mu^\star$ [see Eq. (7)] as a function of the inertial number $I(z)$ computed locally at different depth z for all simulations from sets A, B, and C, in log-log and linear scales; the full line shows $\mu^\star = I/I_0$.

B. Implication for the velocity profiles

As detailed above, relation (6) can be rewritten

$$I(z) = I_0 \mu^\star,$$

$$\frac{dv_x}{dz} = \frac{I_0 \mu^\star}{d}\left[\frac{P(z)}{\rho}\right]^{1/2},$$

where $P \simeq \sigma_{zz} \simeq \rho g (H-z)\cos\theta$. Integrating this gives

$$v_x(z) - v_x(0) = \frac{2}{3} I_0 \mu^\star \cos\theta \frac{g^{1/2}}{d}[H^{3/2} - (H-z)^{3/2}] \qquad (8)$$

consistently with Bagnold rheological model and the corresponding prediction for the velocity profiles. We test the prediction (8) for three example flows from sets A, B, and C, respectively, taking $\mu = \tan(\theta)$ and adjusting the values of μ_m, μ_M, and I_0 (see Fig. 8). The agreement is good, although the examples correspond to rather low values of I.

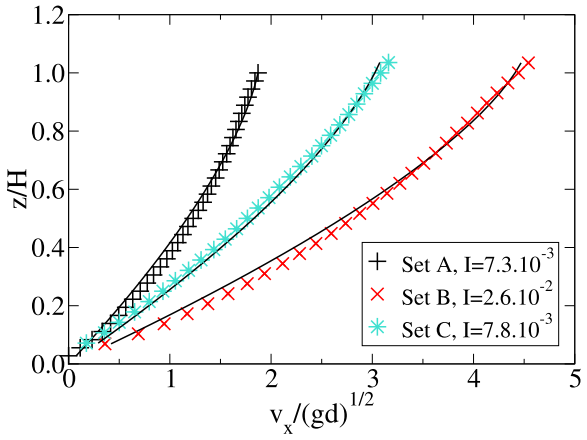

FIG. 8. (Color online) Examples of velocity profiles from sets A, B, and C, and the corresponding predictions following Eq. (8), with $\mu_m = 0.239$, $\mu_M = 0.470$, and $I_0 = 0.133$ for set A, $\mu_m = 0.240$, $\mu_M = 0.650$, and $I_0 = 0.240$ for set B, and $\mu_m = 0.168$, $\mu_M = 0.610$, and $I_0 = 0.237$ for set C.

V. THE PRANDTL MIXING LENGTH APPROACH

In an approach similar to the Bagnold rheology, the Prandtl mixing length approach postulates the existence of a coherence length scale ℓ such that

$$\sigma_{zz} = \rho \ell^2 \left(\frac{\partial v_x}{\partial z}\right)^2. \qquad (9)$$

Beyond the analogy with turbulent layers, the physical origin of this coherence length has to be specified; it is commonly identified with the typical length of grains velocity fluctuations correlations, namely, the typical size of granular eddies or clusters.[11,29] Considering both Eqs. (9) and (2), consistency with the Bagnold rheology implies that

$$\ell/d = \kappa(\phi)^{1/2} = I^{-1}. \qquad (10)$$

Experimental evidence of the existence of correlated motion of grains at the surface of chute flows was given by Ref. 13; the typical correlation length associated was found to be of few grain diameters (up to eight), and its behavior regarding the flow dynamics was consistent with the h_{stop} phenomenology.[1] Numerical evidence of correlated motion in the bulk was later produced.[6,10,12] In the following, we focus on the existence of correlated motion close to jamming. Spatial correlations of grains velocity fluctuations are therefore closely analyzed.

A. Correlation of velocity fluctuations

Each grain in the flow is characterized by its velocity fluctuations $\delta v_x^i = |v_x^i - \langle v_x \rangle|$. Since the amplitude of velocity fluctuations varies in depth,[6] spatial correlations associated to velocity fluctuations are computed at a specified depth $z \pm d/2$. At this given depth, correlation are quantified by a pair correlation function

$$F_{xx}(r) = \frac{\Sigma_{i,j} \delta v_x^i \delta v_x^j \Pi(x_{ij} - r)}{\Sigma_{i,j} \Pi(x_{ij} - r)},$$

where x_{ij} is the distance between the grains i and j, and $\Pi(x_{ij} - r)$ is a step function taking the value 1 where $|x_{ij} - r| < d/2$, and 0 otherwise. Considering three different depth in the flow $z = 10d$, $20d$, and $30d$ for set A, and $z = 7d$, $15d$, and $20d$ for sets B and C, the pair correlation functions are computed for all simulations, and time-averaged over their duration. They show an exponential form $F_{xx}(r) \simeq \exp(-r/\lambda)$, where from we directly evaluate the correlation length λ associated to velocity fluctuations (Fig. 9, inset graph). The correlation length λ is plotted as a function of the inertial number I in Fig. 9. We find, in agreement with previous works,[6,10,12,13] that smaller values of the inertial number coincide with rapidly increasing correlation lengths, namely, that grains have an increasingly correlated motion when reaching close to jamming, forming *granular eddies* as defined by Ref. 11.

We find:

$$\lambda/d \simeq 1.38 I^{-0.32 \pm 0.008}. \qquad (11)$$

We do not observe $\lambda/d \propto I^{-1}$ as expected consistently with the Bagnold model [Eq. (10)]. Interestingly, the scaling (11)

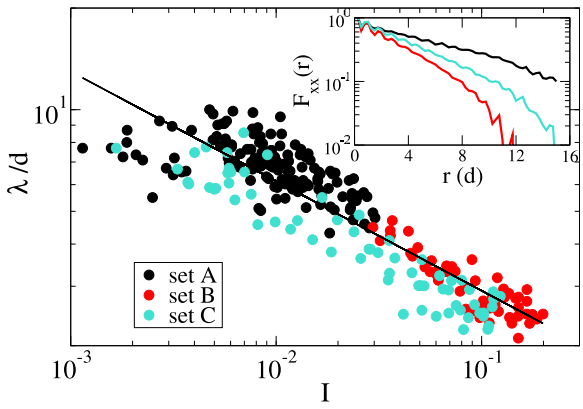

FIG. 9. (Color online) Correlation length λ of grains velocity fluctuations as a function of the inertial number I (computed at $z=10d$, $20d$, and $30d$ for set A, and $z=7d$, $15d$, and $20d$ for sets B and C); the full line shows $\lambda=1.38I^{-0.32}$. Inset graph: examples of the shape of the pair correlation function $F_{xx}(r)$ for sets A, B, and C.

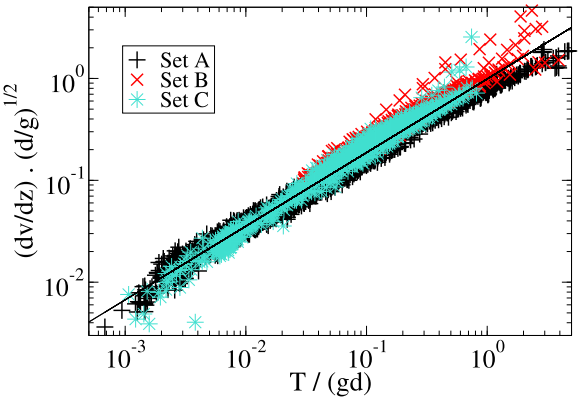

FIG. 11. (Color online) Local value of the normalized velocity gradient $(d/g)^{1/2}(\partial v_x/\partial z)(z)$ for all simulations as a function of the local normalized temperature $T(z)/(gd)$. The straight line shows the power-law trend $(d/g)^{1/2}(\partial v_x/\partial z)(z)=0.99[T(z)/gd]^{0.723}$.

matches recent experimental observation by Ref. 30 in granular heap flows, where the typical size of "dynamical heterogeneities" close to jamming is found to diverge like $I^{-0.33}$.

B. The granular temperature

We define the granular temperature as the square of the mean grains velocity fluctuations:

$$T(z)=\langle(\delta v)^2\rangle=\langle v_x^2\rangle(z)-\langle v_x\rangle^2(z). \tag{12}$$

In most cases, the temperature is maximum at the bottom, which coincides with the fact that the bottom, due to its rigidity, dissipates the energy of the above layer of flowing grains less efficiently then elsewhere in the flow where colliding grains are free to move, unconstrained, in any direction. This is also consistent with the systematic decrease of the volume fraction near the bottom (see Fig. 3). We plot all normalized temperature profiles $T(z)/\langle T\rangle$ in Fig. 10, where $\langle T\rangle$ is the mean temperature averaged over the flow volume, for set A and B and C. We observe that an exponential decay is a possible approximation:

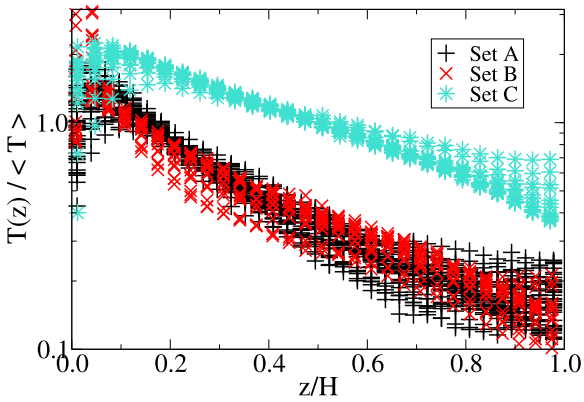

FIG. 10. (Color online) Normalized profiles of the granular temperature $T(z)/\langle T\rangle$ for all simulations from sets A, B and C, where $\langle T\rangle$ is the mean temperature over the volume of the flow.

$$T(z)\simeq T_0\exp\left(-\alpha\frac{z}{d}\right). \tag{13}$$

The best fit approximation gives $\alpha=0.066$ for set A, $\alpha=0.079$ for set B, and $\alpha=0.056$ for set C. The typical length over which temperature decreases, namely, $15d$, $13d$, and $18d$, respectively, is smaller compared to the depth H of the flow ($H=40d$ for set A and $H=32d$ for sets B and C), yet of the same order. It is not clear whether the higher temperature at the bottom is the signature of a boundary layer, or whether it would expand in the bulk of the flow in the case of much thicker bed (large H). This would need to be established in further work.

C. Implications for the velocity profile

Figure 11 shows the shear rate $\partial v_x/\partial z$ plotted as a function of the temperature T for all simulations of sets A, B and C, for all depth z. The relatively good collapse of the data over several orders of magnitude is compatible with a power-law; the best fit gives

$$\frac{\partial v_x}{\partial z}\propto T^{\beta}, \tag{14}$$

with $\beta=0.723\pm0.002$. This scaling is consistent with observation of grains dynamics in annular shear configurations, as well as in simulated plan shear flows.[31,32]

Since temperature profiles are compatible with an exponential decrease [see scaling (13)], the scaling (14) implies that velocity profiles should obey the same trend. Integrating Eq. (14) using relation (13) leads directly to

$$v(z)-v(0)=\frac{v(H)-v(0)}{1-\exp\left(-\gamma\frac{H}{d}\right)}\left[1-\exp\left(-\gamma\frac{z}{d}\right)\right], \tag{15}$$

where $\gamma=\alpha\beta$ is the only one parameter to be adjusted. Considering the same velocity profiles from sets A, B, and C displayed in Fig. 8, we test this new prediction and find a good agreement, with $\gamma=0.045$ for set A and set B and $\gamma=0.032$ for set C (Fig. 12).

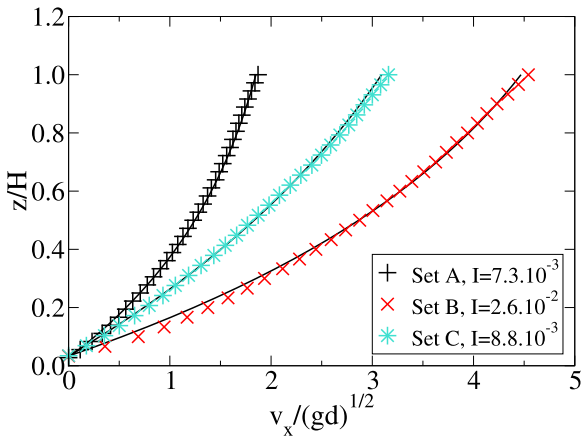

FIG. 12. (Color online) Examples of velocity profiles from sets A, B, and C, and the corresponding prediction using Eq. (15).

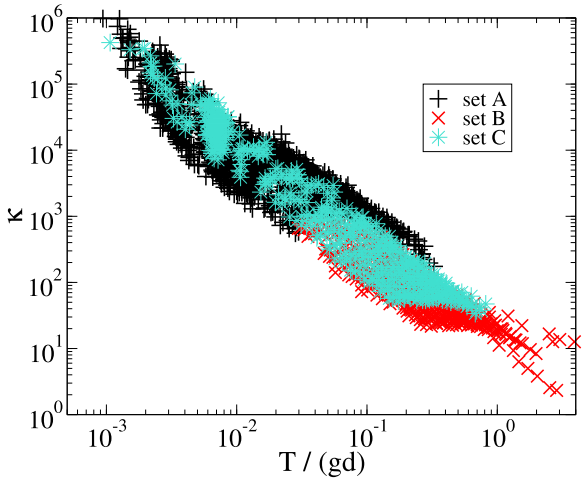

FIG. 14. (Color online) Viscosity function κ defined as $\kappa = \sigma_{zz}/\rho d^2(\partial v_x/\partial z)^2$, computed for all depths z, and plotted as a function of the normalized granular temperature $T(z)/gd$ for all simulations from sets A, Bs and C.

VI. TOWARD A NONLOCAL RHEOLOGY?

In the previous section, we have characterized the existence of a length scale related to grains velocity fluctuations whose dependence on the inertial number suggests the emergence of large scales in the flow close to jamming. Considering the temperature profiles and their correlation with velocity gradients, we were able to predict the shape of the velocity profiles outside the framework of Bagnold's model. At this stage, we can question the role of the granular temperature in the rheology, and more specifically how it links to the effective viscosity, far from the framework of kinetic theory.

A. Viscosity, granular eddies, and temperature

For each simulation, the correlation length λ was computed at three different depths ($z=10d$, $20d$, and $30d$ for set A, and $z=7d$, $15d$, and $20d$ for sets B and C). The effective viscosity $\nu=\sigma_{zz}/(\partial v_x/\partial z)$, computed for the same values of z, is plotted as a function of λ in Fig. 13. A clear trend comes out, giving (with a correlation coefficient of 0.89)

$$\nu/(\rho g^{1/2} d^{3/2}) \simeq 2.11\left(\frac{\lambda}{d}\right)^{2.69\pm0.078}$$

and relating viscosity and the size of "granular eddies."

Remaining in the framework of a Bagnold-like expression for the stress/shear-rate [Eq. (2)], we search for a viscosity function κ which, rather than of the volume fraction ϕ, would be a function of the granular temperature T:

$$\sigma_{zz} = \rho d^2 \kappa(T)\left(\frac{\partial v_x}{\partial z}\right)^2. \tag{16}$$

The plot of the viscosity function κ against T is displayed in Fig. 14: the points do not collapse and spread over one order of magnitude; yet, we observe a well-defined decreasing trend, where lower temperature values coincide with higher viscosity.

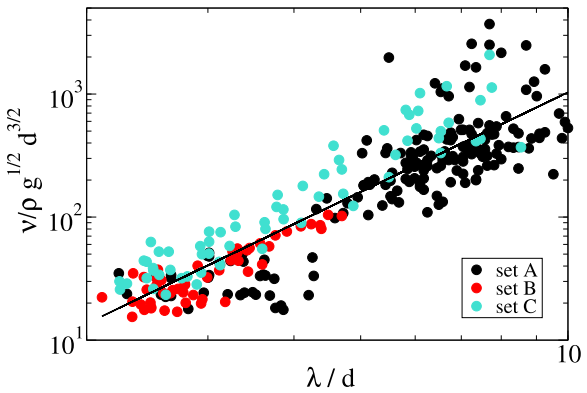

FIG. 13. (Color online) Normalized viscosity $\nu/(\rho g^{1/2} d^{3/2})$, where $\nu=\sigma_{zz}/(\partial v_x/\partial z)$ as a function of the correlation length of velocity fluctuations λ/d. The full line shows $\nu/(\rho g^{1/2} d^{3/2})=2.11(\lambda/d)^{2.69}$.

B. A nonlocal behavior

However, it is possible to make all simulation points merge following a single curve if, instead of considering the local stress $\sigma_{zz}(z)$ only, we consider the stress variation with regard to the bottom $\sigma_{zz}(0)-\sigma_{zz}(z)$ (where $\sigma_{zz}(0)$ is computed from the first layer of grains at the bottom). In this case, the collapse of the points, displayed in Fig. 15, gives (with a correlation coefficient of 0.98)

$$\kappa' \simeq 1.65\left(\frac{T}{gd}\right)^{-1.7\pm0.007}, \tag{17}$$

where κ' is defined as

$$\kappa' = [\sigma_{zz}(0) - \sigma_{zz}(z)]/[\rho d^2(\partial v_x)/\partial z]^2. \tag{18}$$

Interestingly, this collapse extends over several orders of magnitude and does not degrade close to jamming, when $T\to 0$. Since for chute flows, $\sigma_{zz}(0)\simeq \rho g H \cos\theta$ and $\sigma_{zz}(z) \simeq \rho g(H-z)\cos\theta$, the scaling observed can be rewritten

$$\sigma_{zz}(0) - \sigma_{zz}(z) = \rho d^2 \kappa'(T)\left(\frac{\partial v_x}{\partial z}\right)^2,$$

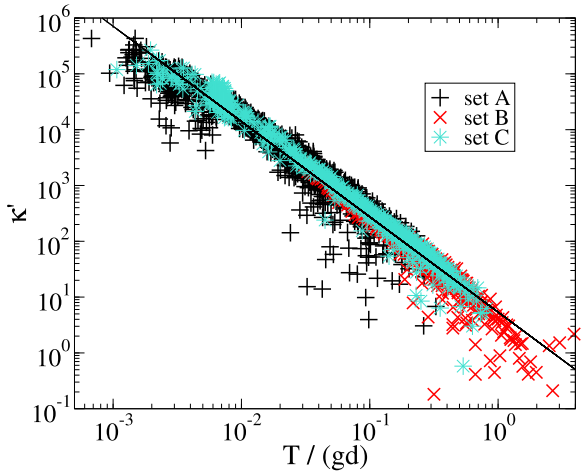

FIG. 15. (Color online) Function κ' defined as $\kappa'=[\sigma_{zz}(0)-\sigma_{zz}(z)]/[\rho d^2(\partial v_x/\partial z)^2]$ and computed for all depths z, plotted as a function of the normalized granular temperature $T(z)/gd$ for all simulations from sets A, B, and C. The full line shows the power-law fit $\kappa'=1.65[T(z)/gd]^{-1.7}$.

$$\sigma_{zz}(z)\left(\frac{H}{H-z}-1\right)\simeq\rho d^2\kappa'(T)\left(\frac{\partial v_x}{\partial z}\right)^2,$$

which leads directly to

$$\sigma_{zz}(z)\simeq\rho d^2\frac{H-z}{z}\kappa'(T)\left(\frac{\partial v_x}{\partial z}\right)^2, \tag{19}$$

where

$$\kappa'(T)\simeq 1.65\left(\frac{T}{gd}\right)^{-1.7}.$$

This correlation suggests the existence of a relation between stress and shear rate involving the distance to the bottom and the distance to the free surface through the length scale $\xi=d\sqrt{(H-z)/z}$. If $z=H$, the stress is zero, as expected at the free surface. If $z\to 0$, ξ diverges, which could only be balanced by the fact that the temperature becomes infinite at the bottom. The relation thus breaks down at the bottom. However, it is still valid for z as small as one grain diameter d, and the scaling (19) actually holds at all depths in our simulations, as can be seen in Fig. 15.

The fact that the stress at the bottom appears in the correlation observed in Fig. 15 stresses the role played by the substrate in chute flow dynamics, and suggests that this role extends to the whole bulk. Everywhere in the bulk, the scaling (19) strongly hints at a nonlocal rheology: local stress does not only depend on the local shear rate but also on the distance to the surface and to the bottom. In our simulations, granular temperature, namely, velocity fluctuations, appears to be at the origin of the nonlocality. Close to jamming, and very far from the framework of kinetic theory where it is given a thermodynamically meaningful interpretation, granular temperature seems to play a fundamental role in the flow behavior.

VII. SUMMARY AND DISCUSSION

In order to test the rheology of granular flows, we have performed series of numerical simulations (90 in total) of nearly monodisperse stationary chute flows from rapid ($I=10^{-1}$) to slow and very slow ($I=10^{-3}$) flow regime, namely, close to the jamming transition. Computing locally quantities such as the stress tensor, the strain rate, the velocity, and the volume fraction allows for a detailed analysis of flows state. The aim was twofold: *(i)* checking how existing rheological models (the Bagnold's model and the *I*-model) capture the behavior of the numerical flows at the verge of the transition to jamming, and *(ii)* performing an acute characterization of the structure of the flow in terms of grains velocity fluctuations at this transition.

Our results show that neither Bagnold's model nor the *I*-model capture the behavior of the numerical points in the slow regime, namely, when $I\leq 2\times 10^{-2}$; in this regime, the huge scattering of the data prevents concluding on the validity of the models. Turning to the analysis of grains velocity fluctuations, we compute the associated correlation length λ and show its dependence on the inertial number: $\lambda/d\propto I^{-0.32}$. The amplitude of the grains velocity fluctuations, namely, the granular temperature, exhibits a power-law dependence on the shear rate and allows for a prediction of the shape of the velocity profiles. The main result consists of a scaling merging all data points for all flow regimes onto the same master curve, and relating granular temperature, shear rate, and the variation of stress between the considered depth and the bottom wall. This scaling can be written as a relation among local stress, local shear rate, and local temperature, provided the introduction of a characteristic length scale $\xi=d\sqrt{(H-z)/z}$ where both the distance to the surface and the distance to the bottom wall are involved. This scaling strongly hints at a nonlocal behavior, valid in the flow regime and extending close to the jamming transition.

While the hypothesis of a nonlocal rheology has long been put forward, and applied recently with success,[22,23] it is often assumed that the mode of stress transmission and the important stress fluctuations observed in granular media are responsible for the nonlocality. However, our results point at the velocity fluctuations as the agent allowing for nonlocal effects. Although weak in amplitude, and far from the framework of kinetic theory, granular temperature could still be an efficient variable to describe granular flow behavior in dense regime.

Our result are limited to the study of model 2D chute flows and the generalization to other flow configurations is far from straightforward. However, the observation of a scaling demonstrating the influence of the bottom wall to the whole bulk of the flow suggests that walls in general might play a more fundamental role in the granular dynamics than simply boundary conditions. This could lay a new basis to understand the puzzling influence walls sometimes exert in granular systems.[28,33]

An obvious continuation of this work will be the study of the influence of the flow depth H on the phenomenology observed, the repercussion on granular temperature, and on the existence of nonlocal effects.[34] Eventually, this would

most likely open new prospects in the understanding of the h_{stop} phenomenology, which is a long discussed token of granular nonlocal rheology.

[1] O. Pouliquen, "Scaling laws in granular flows down rough inclined planes," Phys. Fluids **11**, 542 (1999).
[2] B. Andreotti, A. Daerr, and S. Douady, "Scaling laws in granular flows down a rough plane," Phys. Fluids **14**, 415 (2002).
[3] A. Daerr, "Dynamical equilibrium of avalanches on a rough plane," Phys. Fluids **13**, 2115 (2001).
[4] L. E. Silbert, D. Ertaş, G. S. Grest, T. C. Halsey, D. Levine, and S. J. Plimpton, "Granular flow down an inclined plane: Bagnold scaling and rheology," Phys. Rev. E **64**, 051302 (2001).
[5] D. Bonamy, F. Daviaud, and L. Laurent, "Multiscale clustering in granular surface flows," Phys. Rev. Lett. **89**, 034301 (2002).
[6] L. Staron, "Correlated motion in the bulk of dense granular flows," Phys. Rev. E **77**, 051304 (2008).
[7] I. S. Aranson and L. V. Tsimring, "Continuum theory of partially fluidized granular flows," Phys. Rev. E **65**, 061303 (2002).
[8] J.-P. Bouchaud, M. E. Cates, J. Ravi Prakash, and S. F. Edwards, "Hysteresis and metastability in a continuum sandpile model," Phys. Rev. Lett. **74**, 1982 (1995).
[9] C. Josserand, P.-Y. Lagrée, and D. Lhuillier, "Stationary shear flows of dense granular materials: A tentative continuum modeling," Eur. Phys. J. E **14**, 127 (2004).
[10] P. Mills, P. G. Rognon, and F. Chevoir, "Rheology and structure of granular materials near the jamming transition," Europhys. Lett. **81**, 64005 (2008).
[11] D. Ertaş and T. C. Halsey, "Granular gravitational collapse and chute flow," Europhys. Lett. **60**, 931 (2002).
[12] O. Baran, D. Ertaş, T. C. Halsey, G. S. Grest, and J. B. Lechman, "Velocity correlations in dense gravity-driven granular chute flow," Phys. Rev. E **74**, 051302 (2006).
[13] O. Pouliquen, "Velocity correlations in dense granular flows," Phys. Rev. Lett. **93**, 248001 (2004).
[14] A. V. Orpe and A. Kudrolli, "Velocity correlations in dense granular flows observed with internal imaging," Phys. Rev. Lett. **98**, 238001 (2007).
[15] F. da Cruz, S. Emam, M. Prochnow, J.-N. Roux, and F. Chevoir, "Rheophysics of dense granular materials: Discrete simulation of plane shear flows," Phys. Rev. E **72**, 021309 (2005).
[16] GdR Midi, "On dense granular flows," Eur. Phys. J. E **14**, 341 (2004).
[17] L. Lacaze and R. R. Kerswell, "Axisymmetric granular collapse: A Transient three-dimensional flow test of viscoplasticity," Phys. Rev. Lett. **102**, 108305 (2009).
[18] C. Ancey, P. Coussot, and P. Evesque, "A theoretical framework for granular suspensions in a steady simple shear flow," J. Rheol. **43**, 1673 (1999).
[19] S. B. Savage and K. Hutter, "The motion of a finite mass of granular material down a rough incline," J. Fluid Mech. **199**, 177 (1989).
[20] P. Jop, Y. Forterre, and O. Pouliquen, "A consitutive law for dense granular flows," Nature (London) **441**, 727 (2006).
[21] I. S. Aranson, L. V. Tsimring, F. Malloggi, and E. Clément, "Nonlocal rheological properties of granular flows near a jamming limit," Phys. Rev. E **78**, 031303 (2008).
[22] P. Mills, D. Loggia, and M. Tixier, "Model for a stationary dense granular flow along an inclined wall," Europhys. Lett. **45**, 733 (1999).
[23] O. Pouliquen and Y. Forterre, "A nonlocal rheology for dense granular flows," Philos. Trans. R. Soc. London, Ser. A **367**, 5091 (2009).
[24] M. Jean and J.-J. Moreau, in *Unilaterality and Dry Friction in the Dynamics of Rigid Bodies Collection*, edited by A. Curnier (Presses Polytechniques et Universitaires Romandes, Lausanne, 1992), pp. 31–48.
[25] J.-J. Moreau, "Some numerical methods in multibody dynamics: Application to granular materials," Eur. J. Mech. A/Solids **4**, 93 (1994).
[26] L. Staron and E. J. Hinch, "Study of the collapse of granular columns using 2D discrete-grains simulation," J. Fluid Mech. **545**, 1 (2005).
[27] P. Eshuis, K. van der Weele, D. van der Meer, and D. Lohse, "Granular Leidenfrost effect: Experiment and theory of floating particles clusters," Phys. Rev. Lett. **95**, 258001 (2005).
[28] P. Jop, Y. Forterre, and O. Pouliquen, "Crucial role of side walls for granular surface flows: consequences for the rheology," J. Fluid Mech. **541**, 167 (2005).
[29] G. Debrégeas and C. Josserand, "A self-similar model for shear flows in dense granular materials," Europhys. Lett. **522**, 137 (2002).
[30] H. Katsuragi, A. R. Abate, and D. J. Durian, "Jamming and growth of dynamical heterogeneities versus depth in granular heap flow," Soft Matter **13**, 3038 (2010).
[31] W. Losert, L. Bocquet, T. C. Lubensky, and J. P. Gollub, "Particle dynamics in sheared granular matter," Phys. Rev. Lett. **85**, 1428 (2000).
[32] N. Xu, C. S. O' Hern, and L. Londic, "Stabilization of no-linear velocity profiles in athermal systems undergoing planar shear flow," Phys. Rev. E **72**, 041504 (2005).
[33] N. J. Balmforth and R. R. Kerswell, "Granular collapse in two dimensions," J. Fluid Mech. **538**, 399 (2005).
[34] C. Bonnoit, J. Lanuza, A. Lindner, and E. Clément, "Mesoscopic length scale controls the rheology of dense suspensions," Phys. Rev. Lett. **105**, 108302 (2010).